

Classical noise, Quantum noise and Secure communication

C. Tannous and J. Langlois

Laboratoire de Magnétisme de Bretagne - CNRS FRE 3117

UBO, C.S.93837 - 29238 Brest Cedex 3 - FRANCE

(Dated: September 19, 2016)

Secure communication based on message encryption might be performed by combining the message with controlled noise (called pseudo-noise) as performed in Spread-Spectrum communication used presently in Wi-Fi and Smartphone Telecommunication systems. Quantum communication based on entanglement is another route for securing communications as demonstrated by several important experiments described in this work. The central role played by the photon in unifying the description of Classical and Quantum noise as major ingredients of secure communication systems is highlighted and described on the basis of the classical and quantum fluctuation dissipation theorems.

I. INTRODUCTION

Secure communication based on message encryption with controlled noise (pseudo-noise or PN) started with the work of the actress-engineer Hedy Lamarr and her husband-pianist Georges Antheil in 1941 who were interested in military communications during World War II.

Lamarr invented frequency hopping to prevent an intruder from jamming a signal sent to control torpedoes remotely, since using a single frequency might be easily detected and blocked. Frequency hopping is used presently in Bluetooth and other types of wireless communication and is called FHSS¹ (Frequency Hopping Spread Spectrum).

Given a set of frequency values $[f_1, f_2, f_3, \dots]$, one selects a well-defined sequence of frequencies following an apparently random pattern (picked from PN values) shared solely between transmit and receive ends. For an eavesdropper unaware of the sequence used, the signal appears as white noise containing no valuable information and that is the reason why it is termed spread-spectrum communication given that noise has broader bandwidth than the signal.

FHSS needs another important ingredient to be completely operational: sender-receiver perfect synchronization in order to be able to modulate-demodulate with the right frequency. It is Antheil, exploiting his musician skills, who developed the synchronization¹ method between sender and receiver enabling them to encrypt-decrypt ongoing transmitted information.

The analog to digital conversion of frequency hopping gave birth to DSSS (Direct Sequence Spread Spectrum) methods based on Galois polynomials, the generators of PN sequences that we describe below and that are used presently in Wi-Fi and other types of digital communications (Smartphones...).

Consequently, it is important to relate noise to communications, how it might be used to alter the nature of the signal and ultimately transmit hidden information in a way such that it is properly retrieved by the target receiver.

An ordinary resistor has a fluctuating voltage across it

whether standing free or belonging to an electronic circuit. The resistor embodies free electrons that are thermally agitated, inducing random voltage fluctuations.

Most physicists/engineers refer to this thermal voltage fluctuation as Johnson-Nyquist noise, after J.B. Johnson², who was first to observe the effect at Bell laboratories in 1928 and H. Nyquist² who first explained it.

Circuit noise studies in Bell laboratories have a very peculiar history since in the 1950's, H. E. D. Scovil and his associates built the world's lowest-noise microwave amplifiers cooled by liquid helium to reduce noise and incorporated in extremely sensitive radiometers used in radio-astronomy.

Radiometers usually contain calibration noise sources consisting of a resistor at a known temperature. During the 1960's Penzias and Wilson³ while improving these radiometers discovered serendipitously Big-Bang cosmic background radiation in 1965.

B. Yurke⁴ and his collaborators embarked, in the 1980's, on a pioneering study of Quantum noise through the quantization of LC networks drawing from an analogy between an LC circuit and the harmonic oscillator. Quantum effects in circuits occur when we deal with low temperature (as in superconductors) or at very high frequency. Usual telecommunication and signal processing frequencies are in the kHz-GHz range whereas Tera-Hz (10^{12} Hz) devices encountered in medical imaging and optical devices operate at 10^{14} Hz. Consequently, kHz-GHz frequencies are classical whereas Tera-Hz and optical devices should be considered as quantum. With the progress of integrated circuits toward the nanometer scale (presently the minimal feature used in the semiconductor industry is 14 nm) and single electron as well as quantum dot (akin to synthetic atom) devices, we expect large quantum effects implying quantum noise becoming more important than thermal.

The equivalence between an impedance and an oscillator is a very important idea that will trigger and sustain steady progress in several areas of Quantum information and communication.

Nyquist derived an expression for White Noise based on the interaction between electrons and electromagnetic waves propagating along a transmission line using arguments based on black-body radiation. This means that

Nyquist is in fact a true pioneer in Quantum noise.

He based his work on Johnson measurements who found that thermal agitation of electricity in conductors produces a random voltage variation between the ends of the conductor R of the form:

$$\langle (V - \langle V \rangle)^2 \rangle = \langle \delta V^2 \rangle = 4Rk_B T \Delta f \quad (1)$$

$\langle \dots \rangle$ is the average value, voltage fluctuation is $\delta V = V - \langle V \rangle$ and V is the instantaneous voltage measured at the ends of the resistance R . k_B is Boltzmann constant and T is absolute temperature. Δf is the bandwidth of voltage fluctuations (see Appendix A). This frequency interval spans the range of a few Hz to several tens of GHz.

The voltage fluctuation developed across the ends of the conductor due to Thermal noise is unaffected by the presence or absence of direct current. This can be explained by the fact that electron thermal velocities in a conductor are much greater ($\sim 10^3$ times) than electron drift velocities.

Since electromagnetic waves are equivalent to photons through Quantum Mechanics Duality principle⁵, Nyquist derivation is based on blackbody radiation that was explained earlier by Planck.

In Quantum Mechanics language, a (zero rest mass) photon is a special case of a harmonic oscillator since the energy levels are separated by the same energy $\hbar\omega$ i.e. the n -th level $E_n = n\hbar\omega$ (ignoring zero-point energy $\hbar\omega/2$) corresponds to an integer number n of photons. Moreover $\omega = 2\pi f$ is the electromagnetic pulsation and not the mechanical one $\sqrt{k/m}$ where k, m are the respective spring constant and mass of the mechanical oscillator.

While classical pseudo-noise used in spread-spectrum communications hides the signal from intrusion by an eavesdropper through a crypting operation (FHSS frequencies follow a PN sequence whereas in DSSS, the signal is directly multiplied by the PN sequence) using a set of keys (corresponding to a given PN sequence) that are shared solely between the transmitter and the receiver, Quantum mechanics can be used to encrypt the signal in a completely different fashion.

Quantum Mechanics can be used to generate naturally random instead of deterministic pseudo-random numbers. In the early days of computing cosmic rays or radioactive sources⁶ were used for generating non-deterministic random numbers. Quantum phenomena being essentially non-deterministic, would be able to produce truly random numbers and the corresponding devices are called Quantum Random Number Generators⁶ (QRNG).

Obviously, this is not the only advantage of Quantum Mechanics since at the Garching Max Planck Institute for Quantum Optics (MPQ) in Germany and the Technical University of Vienna, communication experiments showed that Quantum Mechanics provides entanglement as an alternative concept to secure information transfer between two remote sites.

Entanglement, first introduced by Einstein (who called it "spooky action at a distance"), Podolsky, and Rosen⁷, and Schrödinger⁸ in 1935, can arise when two quantum systems are produced from a common source, e.g. when a spinless particle decays into two particles carrying opposite spins. Such states violate a set of inequalities⁹ established by J.S. Bell in 1964, implying that quantum theory embodies non-locality (see section IV for the mathematical implication). Bell inequalities are the statistical measure of entanglement and their violation can be demonstrated by measuring correlations between quantum states.

Entangled quantum systems behave as if they can affect each other instantaneously, even when they are extremely far from each other, due to the essential non-local¹⁰ character of entanglement.

The strongest advantage of noise-based communication is that by hiding a signal in noise, it is extremely difficult or even impossible to detect it if the eavesdropper does not know the keys or the algorithm used between the transmitter and the receiver. In Quantum communication (QC), entanglement ties together in a very stringent fashion both parties and any intrusion attempted by an eavesdropper, when detected, triggers immediately disruption of communication.

This work can be taught as an application chapter in a general Statistical Physics course at the Graduate or in a specialized Graduate course related to applications of Quantum Mechanics and Statistical Physics since physicists generally interested in the applications of Quantum Mechanics and Statistical Physics are keen to expand their knowledge to areas of Quantum Information Processing and Communications (QIPC).

This paper is organized as follows: after reviewing several derivations of White noise by Nyquist and others in section II, we discuss in section III the Fluctuation Dissipation theorem and its quantum version in order to derive in a rigorous way, Nyquist result with modern quantum noise approach and lay the foundations of secure communication from the classical and quantum points of view. In section IV we apply the analysis to secure communications with classical noise (spread-spectrum) and entanglement based Quantum information processing and transfer. Discussions and Conclusions are in section V.

II. DERIVATIONS OF THERMAL NOISE

Nyquist work is based on phenomenological thermodynamic considerations and electric circuit theory, including the classical equipartition theorem. The latter is based on the physical system number of degrees of freedom. This number¹¹ is well defined when the different contributions to system energy (translational, rotational, vibrational, electromagnetic...) are quadratic and decoupled with presence of weak interactions. In the general case (non-quadratic energy or strong interactions), one evaluates the partition function in order to derive ther-

modynamical properties.

A. Nyquist derivation of Thermal Noise

Nyquist based his derivation on Einstein remark that many physical systems would exhibit Brownian motion and that Thermal noise in circuits is nothing more than Brownian motion of electrons due to ambient temperature. Despite the fact one might find several strange assumptions and even flaws in Nyquist derivation, it remains a pioneering interesting approach since it paves the way to quantization of electrical circuits and noise in circuits. Nyquist considered thermal noise in a resistor R as stemming from electrons interacting with electromagnetic waves represented by a one-dimensional black-body thermal radiator. Electromagnetic waves travel through an ideal (lossless) one-dimensional transmission line of length ℓ joining two resistances R . Hence the transmission line characteristic impedance being equal to R amounts to considering that its impedance is matched at both ends and that any voltage wave propagating along the line is completely absorbed by the end resistor R without any reflection, exactly like a black-body.

Each resistor R has a thermally-fluctuating voltage at temperature T which will be transmitted down the wires with a current and voltage wave appearing across the other resistor.

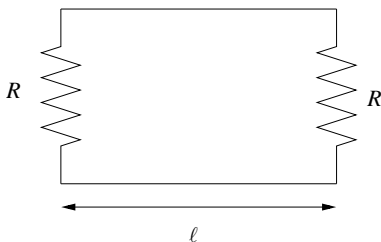


FIG. 1. Transmission line of length ℓ matched by two resistors R at its ends.

A voltage wave propagating along the transmission line is expressed at any point x and any time t as: $V(x, t) = V_0 \exp[i(\kappa x - \omega t)]$ where κ is the wavenumber and ω the angular frequency of the wave.

The velocity $v = \omega/\kappa$ in the line is typically $c/10$ where c is light velocity in vacuum. Considering the transmission line of length ℓ as a domain between $x = 0$ and $x = \ell$ and imposing the boundary condition $V(\ell, t) = V(0, t)$, $\forall t$, we infer that possible propagating wavenumbers are given by $\kappa\ell = 2n\pi$, where n is any integer, and there are $\Delta n = (1/2\pi)d\kappa = d\omega/(2\pi v)$ such modes per unit length of the line in the frequency range between ω and $\omega + d\omega$.

In the Canonical ensemble, the Bose-Einstein distribution for photons gives the mean number of photons $\langle n \rangle$ per mode at energy $\hbar\omega$ and temperature T as:

$$\langle n \rangle = \frac{1}{e^{\beta\hbar\omega} - 1} \quad (2)$$

$\beta = \frac{1}{k_B T}$ is inverse temperature¹² coefficient. Thus the energy of the photon gas (ignoring zero-point energy) is $\langle n \rangle \hbar\omega$.

Detailed balance allows to equate the power absorbed by a resistor (in any angular frequency range ω and $\omega + d\omega$) to the power emitted by it. The energy in the interval ω and $\omega + d\omega$ is proportional (see Appendix C) to the number of propagating modes per unit length in this frequency range. The mean energy per unit time incident upon a resistor in this frequency range is:

$$P_{in} = v \left(\frac{d\omega}{2\pi v} \right) E(\omega) = \frac{1}{2\pi} E(\omega) d\omega \quad (3)$$

where $E(\omega)$ is the electromagnetic energy at ω . Nyquist considers that the total resistance making the circulating current I is $2R$ and thus $I = V/2R$ as if the line whose characteristic impedance R did not contribute at all to the total resistance. Perfect matching at both ends implies that no resistance is contributed by the line since current/voltage waves are not subjected to scattering. The mean power emitted down the line and absorbed by the resistor at the other end is

$$R\langle I^2 \rangle = R \left\langle \frac{V^2}{4R^2} \right\rangle = \frac{1}{4R} \int_0^\infty S_V(\omega) d\omega \quad (4)$$

where S_V is the voltage Power Spectral Density (PSD) (see Appendix A).

Hence we have:

$$\frac{1}{2\pi} E(\omega) d\omega = \frac{1}{4R} S_V(\omega) d\omega \quad (5)$$

with:

$$S_V(\omega) = \frac{2R}{\pi} \frac{\hbar\omega}{e^{\beta\hbar\omega} - 1} \quad (6)$$

Moving from angular to linear frequency, we get:

$$S_V(f) = 4R \frac{hf}{e^{\beta hf} - 1} \quad (7)$$

Voltage fluctuations are given by (see Appendix A):

$$\sigma_V^2 = \langle \delta V^2 \rangle = \int_0^\infty 4R \frac{hf}{e^{\beta hf} - 1} df \quad (8)$$

Performing a change of variable $x = \beta hf$, we get:

$$\sigma_V^2 = \frac{4R(k_B T)^2}{h} \int_0^\infty \frac{x}{e^x - 1} dx \quad (9)$$

Using the integral^{13,14}:

$$\int_0^{\infty} \frac{x^{2n-1}}{e^x - 1} dx = \frac{(2\pi)^{2n} B_n}{4n} \quad (10)$$

with B_n the Bernoulli polynomial coefficients, we select $n = 1$ and $B_1 = \frac{1}{6}$.

The value of the integral in eq. 9 is thus $\frac{\pi^2}{6}$.

The fluctuations are then given by:

$$\sigma_V^2 = \frac{2R(\pi k_B T)^2}{3h} \quad (11)$$

This surprising result implies that, in the classical case, ($h \rightarrow 0$), fluctuations become extremely large. In fact, ordinary frequencies $f \sim \text{kHz-GHz}$ are low with respect to 6.25×10^{12} Hz frequencies that correspond to thermal room temperature energy $k_B T$. Thus $hf \ll k_B T$ and the number of photons per mode is large since $\langle n \rangle \approx k_B T / hf$. In the classical limit, the number of photons being very large, we get wave-like behaviour whereas in the quantum limit a small $\langle n \rangle$ produces particle-like (photon) behaviour.

Expanding the PSD eq.7 at low frequency $hf \ll k_B T$:

$$S_V(f) \approx 4Rk_B T \left(1 - \frac{hf}{2k_B T}\right) \quad (12)$$

Thus quantum effects no longer intervene in the low frequency limit $f \rightarrow 0$, yielding Nyquist result:

$$S_V(0) = 4Rk_B T \quad (13)$$

Another divergence is encountered when we ignore the frequency dependence of $S_V(f)$ in eq. 7 and consider $S_V(0)$ to be valid for all frequencies as usually considered for "White Noise" (flat spectrum for all frequencies):

$$\sigma_V^2 = \int_0^{\infty} 4Rk_B T df = 4Rk_B T \int_0^{\infty} df = \infty \quad (14)$$

This divergence is similar to the Ultra-Violet catastrophe encountered in black-body radiation since $hf \ll k_B T$ corresponds to Rayleigh-Jeans regime and its solution is that voltages are filtered and we never encounter in practice an infinite frequency domain.

Therefore let us assume we have a finite bandwidth Δf for voltage fluctuations, then:

$$\sigma_V^2 = \int_0^{\Delta f} 4Rk_B T df = 4Rk_B T \Delta f \quad (15)$$

To sum up, in order to recover the Johnson-Nyquist result we have to respect two conditions: finite band $\Delta f < \infty$ and low frequencies (kHz-GHz range) $\Delta f \ll k_B T / h$.

Additionally, it is surprising to note that Nyquist considered a 1D photon gas with a single polarization despite the fact the photon had two polarizations (circular left and right) and in sharp contrast with the evaluation of the blackbody radiation by Planck who considered a 3D gas with two polarizations (see Appendix C). Moreover, Nyquist ignored zero-point energy in spite of its importance in quantum circuits and the fact Planck introduced it in his second paper on black-body radiation (see further below).

B. RC circuit classical derivation of Thermal Noise

Nyquist's theorem can be proven with the help of a parallel RC circuit containing a random source representing interactions with a thermal reservoir. The resistor R is parallel to the capacitor C and the result of random thermal agitation of the electrons in the resistor will charge and discharge the capacitor in a random fashion.

Starting from the time dependent equation of motion of the RC circuit, we have:

$$R \frac{dq(t)}{dt} = -\frac{q(t)}{C} + \xi(t) \quad (16)$$

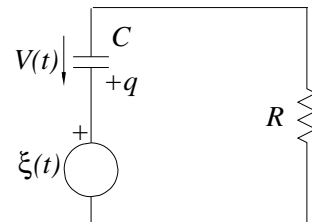


FIG. 2. RC circuit with the noise source $\xi(t)$ originating from thermal contact with a reservoir.

$q(t)$ is the capacitor charge and $\xi(t)$ is a stochastic voltage (see Appendix A) stemming from interactions with a reservoir at temperature T with the following statistical properties:

$$\langle \xi(t) \rangle = 0 \text{ and } \langle \xi(t)\xi(t') \rangle = \lambda \delta(t - t') \quad (17)$$

λ is a constant that will be determined later and eq. 16 is called a Langevin equation¹⁵ (see Appendix B) due to the presence of the time-dependent random term $\xi(t)$.

Assuming the capacitor is uncharged at time $t = -\infty$, direct integration of the first-order differential equation yields:

$$q(t) = \frac{1}{R} \exp(-t/RC) \int_{-\infty}^t \exp(t'/RC) \xi(t') dt' \quad (18)$$

The voltage $V(t)$ across the capacitor is related to charge through: $q(t) = CV(t)$, therefore evaluating the charge PSD (see Appendix A) is equivalent to voltage PSD.

Using properties of $\xi(t)$ given in eq. 17, we obtain:

$$\langle q(t)q(t') \rangle = C^2 \langle V(t)V(t') \rangle = \frac{\lambda C}{R} \exp\left(-\frac{|t-t'|}{RC}\right) \quad (19)$$

This result is expected as discussed in Appendix A since the auto-correlation $\langle q(t)q(t') \rangle$ must be a decreasing function of the argument $|t-t'|$ controlled by the relaxation time RC .

Setting $t = t'$ we have the equality: $C^2 \langle V^2(t) \rangle = \frac{\lambda C}{R}$, hence λ is determined as: $\lambda = RC \langle V^2(t) \rangle$.

The average $\langle V^2(t) \rangle$ can be determined from the energy $\frac{1}{2}C \langle V^2 \rangle$ stored in the capacitor through the classical equipartition theorem: $\frac{1}{2}C \langle V^2 \rangle = \frac{1}{2}k_B T$ as if a capacitor is equivalent to a single degree of freedom (see next section).

The equipartition theorem can be proven as follows. If a system is at temperature T , the probability that it is in a state of energy E is proportional to the Boltzmann factor $\exp(-E/k_B T)$.

In the RC circuit the probability element dp of finding a voltage between V and $(V + dV)$ is $dp = A \exp(-E/k_B T) dV$ corresponding to an energy $E = \frac{1}{2}CV^2$ stored in the capacitor C .

The prefactor A normalizes the probability density:

$$\int_{-\infty}^{\infty} A e^{(-CV^2/2k_B T)} dV = 1 \quad (20)$$

Using the result $\int_{-\infty}^{\infty} e^{-x^2} dx = \sqrt{\pi}$ we get $A = \sqrt{\frac{C}{2\pi k_B T}}$.

The mean square value of the voltage is obtained from the probability density as:

$$\langle V^2 \rangle = A \int_{-\infty}^{\infty} V^2 e^{(-CV^2/2k_B T)} dV \quad (21)$$

Thus $\langle V^2 \rangle = \frac{k_B T}{C}$.

The voltage fluctuation PSD may be evaluated with the equipartition theorem as:

$$S_V(\omega) = \langle V^2 \rangle \frac{2RC}{1 + (RC\omega)^2} = \frac{2Rk_B T}{1 + (RC\omega)^2} \quad (22)$$

At frequencies such that $\omega \ll 1/RC$ we get $S_V(\omega) = 2Rk_B T$ recovering the Johnson-Nyquist result (see note¹⁶).

C. Derivation of Thermal noise from Einstein thermodynamic fluctuation theory

A macroscopic system at thermodynamic equilibrium is an ensemble of subsystems which are in thermodynamic equilibrium with each other. The actual values of the variables, however, may differ from mean equilibrium values.

The departure from equilibrium is due to fluctuations in the subsystems.

The probability, p , for entropy fluctuation δS is obtained by reverting Boltzmann principle $S = k_B \ln W$ as $p(\delta S) = p(S - \langle S \rangle) \propto e^{\delta S/k_B}$. The probability p is proportional to W the number of microscopic available states and we assume the validity of applying Boltzmann principle to the entropy fluctuation δS .

Generally, entropy is a function of state variables X_i , i.e. $S = S(X_1, X_2, \dots, X_i, \dots)$. It can be expanded as dS around equilibrium since it is an analytical function for most thermodynamic systems when small fluctuations of the X_i are considered.

At equilibrium S is maximum and all the first order derivatives $\frac{\partial S}{\partial X_i} = 0, \forall i$ implying that the first non-vanishing terms are quadratic.

Thus one has around equilibrium:

$$\delta S \approx \frac{1}{2} \sum_{i,j} \frac{\partial^2 S}{\partial X_i \partial X_j} \delta X_i \delta X_j \quad (23)$$

The series expansion is performed at the equilibrium value of X_i , hence $\delta X_i = X_i - \langle X_i \rangle$.

The combination of Boltzmann principle and second-order expansion of entropy about equilibrium results in a Gaussian probability density function (PDF) for finding subsystems with the non-equilibrium value of the variable X_i (akin to the central limit-theorem),

$$p(\delta X_i) = \frac{1}{\sqrt{2\pi\sigma_i^2}} e^{-\frac{\delta X_i^2}{2\sigma_i^2}} \quad (24)$$

meaning that the average value (or macroscopic equilibrium) of X_i is $\langle X_i \rangle$ and that the standard deviation away from equilibrium is $\sigma_i^2 = \langle \delta X_i^2 \rangle = -k_B / (\frac{\partial^2 S}{\partial X_i^2})$.

The entropy of a single phase, one component system is given in terms of the energy U , volume Φ and pressure P as $dS = \frac{dU}{T} + \frac{P}{T} d\Phi$.

In the presence of a voltage V , the entropy expression becomes $dS = \frac{dU}{T} + \frac{P}{T} d\Phi - \frac{q}{T} dV$ since charge q couples to voltage V . This yields the value of the entropy derivative $(\frac{\partial S}{\partial V})_{T,\Phi} = -\frac{q}{T}$. The second derivative is thus obtained as: $(\frac{\partial^2 S}{\partial V^2})_{T,\Phi} = -\frac{1}{T} (\frac{\partial q}{\partial V})_{T,\Phi}$.

The voltage fluctuation is expressed as:

$$\sigma_V^2 = \langle \delta V^2 \rangle = -k_B / \left(\frac{\partial^2 S}{\partial V^2} \right)_{T,\Phi} = k_B T \left(\frac{\partial V}{\partial q} \right)_{T,\Phi} \quad (25)$$

Assuming the validity of Ohm's law: $I = \frac{dq}{dt} = \frac{V-V_0}{R}$ where V_0 is some reference voltage (e.g. $V_0 = \langle V \rangle$), we infer that voltage fluctuations are given by:

$$\sigma_V^2 = k_B T R \frac{[d(V - V_0)/dt]}{(V - V_0)} \quad (26)$$

Estimating the time derivative: $\frac{d(V-V_0)}{dt} \sim \frac{(V-V_0)}{\tau}$ with τ as a typical time variation of the voltage and given that for a band-limited signal of bandwidth¹ Δf with $\Delta f \sim \frac{1}{2\tau}$, we finally obtain for the voltage fluctuation expression :

$$\sigma_V^2 = 2Rk_B T \Delta f \quad (27)$$

that agrees with Johnson-Nyquist result (see note¹⁶).

III. THE QUANTUM FLUCTUATION-DISSIPATION THEOREM (QFDT)

The classical fluctuation-dissipation theorem derived in Appendix B provides a relation between equilibrium fluctuations and dissipative transport coefficients. Besides, it is an interesting route to quantize classical noise.

Callen and Welton¹⁷ proved the QFDT with the correspondence theorem allowing to transpose classical results to quantum ones such that a classical physical quantity is transformed into its quantum counterpart with an observable operator.

For a single degree of freedom, linear response theory¹⁸ yields for the change of the expectation value of an operator-valued observable B due to the action of a (classical) force $F(t)$ that couples to the conjugate dynamical operator A :

$$\langle \delta B(t) \rangle = \int_{-\infty}^t ds \chi_{BA}(t-s) F(s). \quad (28)$$

$\delta B(t) = B(t) - \langle B \rangle_0$ denotes the difference with respect to the thermal equilibrium average $\langle B \rangle_0$ in force absence. The dissipative part of the response function $\chi_{BA}(t)$ is given by:

$$\chi_{BA}^D(t) = \frac{1}{2t} [\chi_{BA}(t) - \chi_{AB}(-t)]. \quad (29)$$

The fluctuations are described by the equilibrium correlation function

$$C_{BA}(t) = \langle \delta B(t) \delta A(0) \rangle_\beta \quad (30)$$

The thermal average is taken at an inverse temperature β (see Appendix A).

The correlation function is complex-valued because the operators $B(t)$ and $A(0)$ in general do not commute. While the antisymmetric part of $C_{BA}(t)$ is directly related to the response function by linear response theory, the symmetrized correlation function PSD:

$$S_{BA}(t) = \frac{1}{2} \langle \delta B(t) \delta A(0) + \delta A(0) \delta B(t) \rangle \quad (31)$$

depends on the Fourier transform of the dissipative part of the response function:

$$S_{BA}(\omega) = \hbar \coth \left(\frac{\beta \hbar \omega}{2} \right) X_{BA}^D(\omega). \quad (32)$$

where $X_{BA}^D(\omega)$ is the Fourier transform of $\chi_{BA}^D(t)$. This is the quantum version of the fluctuation-dissipation theorem as it links the fluctuations $S_{BA}(\omega)$ to dissipation as in the classical case (Appendix B).

Note that S_{BA} is a two variable extension of the PSD previously used and defined in Appendix A with a single variable. Consequently S_V should be written in fact as S_{VV} .

Analyzing the response of a current δI through an electric circuit subject to a voltage change δV , implies $B = I$ and $A = Q$, since voltage couples to charge Q .

A circuit response is determined by $\delta I(\omega) = Y(\omega) \delta V(\omega)$ where $Y(\omega)$ is the admittance. Given $I = \dot{Q}$, the symmetrized current PSD is $S_{II}(\omega) = i\omega S_{IQ}(\omega)$ yielding:

$$\begin{aligned} S_{II}(\omega) &= \hbar \omega \coth \left(\frac{\beta \hbar \omega}{2} \right) \Re Y(\omega) \\ &= 2(\langle n \rangle + \frac{1}{2}) \hbar \omega \Re Y(\omega). \end{aligned} \quad (33)$$

where $\langle n \rangle$ is the Bose-Einstein factor (given by eq. 2) and \Re is real part symbol. In the high temperature limit $k_B T \gg \hbar \omega$, we recover the Johnson-Nyquist result $S_{II}(\omega) = 2 \Re Y(\omega) k_B T$ (see note¹⁶).

Nyquist, in the last paragraph of his 1928 paper², had already anticipated the quantum case. However, he made use of Planck first paper on black-body radiation which does not contain zero-point energy term $\frac{1}{2} \hbar \omega$. By missing this term, Nyquist ignored the 1912 second¹⁹ paper on black-body radiation by Planck who aimed at correcting his previous work by introducing zero-point energy in order to recover the right classical²⁰ limit of an oscillator mean energy per mode. Let us add that zero-point energy can also be shown to originate from Heisenberg uncertainty as in the 1D harmonic oscillator case²¹.

If the oscillator mean energy per mode is taken as $\langle n \rangle \hbar \omega$, we obtain to order $O(\frac{1}{k_B T})$ the classical (high temperature) limit $k_B T \gg \hbar \omega$:

$$\begin{aligned} \langle n \rangle \hbar \omega &\approx \frac{\hbar \omega}{1 + \frac{\hbar \omega}{k_B T} + \frac{1}{2} \left(\frac{\hbar \omega}{k_B T} \right)^2 \dots - 1} \\ &\approx \frac{k_B T}{1 + \frac{1}{2} \left(\frac{\hbar \omega}{k_B T} \right) \dots} \approx k_B T - \frac{1}{2} \hbar \omega. \end{aligned} \quad (34)$$

Thus one should rather write the mean energy per mode as $(\langle n \rangle + \frac{1}{2})\hbar\omega$ in order to retrieve the right classical limit $k_B T$ originating from the comparison between Planck photon spectral density expression $\frac{2\omega^2}{\pi^2 c^3} \left[\frac{\hbar\omega}{e^{\beta\hbar\omega} - 1} \right]$ and Rayleigh-Jeans²² expression $\frac{2\omega^2}{\pi^2 c^3} [k_B T]$ (c is the velocity of light).

A. LC circuit quantum derivation of Thermal Noise

We start with an analogy²³ between the harmonic oscillator and the LC resonator. Moving from an RC to an LC circuit stems from the fact a resistance may be defined from $R = \sqrt{\frac{L}{C}}$ and that an oscillator underlying a resistor allows a ready route to quantization.

Later on when we consider a semi-infinite transmission line with L inductance and C capacitance per unit length, the line resistance $R = \sqrt{\frac{L}{C}}$ is same as the single LC resonator. Thus the transmission line might be viewed simply as a large collection of harmonic oscillators (normal modes) and hence can be readily quantized. The resistance picture that links the resonator to the transmission line is very appealing and has been introduced for the first time by Caldeira and Leggett²³ to describe a continuum as sets of harmonic oscillators as described below.

Let us write the Hamiltonian of a single LC resonator circuit in the form:

$$\mathcal{H}_0 = \frac{q^2}{2C_0} + \frac{\phi^2}{2L_0} \quad (35)$$

where variables q and ϕ are capacitor charge and flux in the inductor. Drawing from complete analogy with the harmonic oscillator, we quantize variables with:

$$q = \sqrt{\frac{\hbar}{2R}}(a + a^\dagger), \phi = -i\sqrt{\frac{\hbar R}{2}}(a - a^\dagger) \quad (36)$$

where $R = \sqrt{\frac{L_0}{C_0}}$ and a^\dagger, a are ladder operators characterized by commutation property: $[a, a^\dagger] = 1$.

The Hamiltonian is transformed into standard harmonic oscillator form $\mathcal{H}_0 = \hbar\omega_0(a^\dagger a + \frac{1}{2})$ with $\omega_0 = 1/\sqrt{L_0 C_0}$, the classical resonance frequency.

Moving from a single oscillator to a continuum, we follow Goldstein²⁴ treatment by considering a transmission line of length ℓ characterized by an inductance L and capacitance C per unit length.

The Hamiltonian of the system is

$$\mathcal{H}(t) = \int_0^\ell dx \left[\frac{q^2(x, t)}{2C} + \frac{\phi^2(x, t)}{2L} \right], \quad (37)$$

where $\phi(x, t)$ is the local flux density and $q(x, t)$ is the local charge density.

We define a new variable

$$\theta(x, t) = \int_0^x dx' q(x', t) \quad (38)$$

to express current density $j(x, t) = -\frac{\partial\theta(x, t)}{\partial t}$ and charge density $q(x, t) = \frac{\partial\theta(x, t)}{\partial x}$ such that charge conservation rule:

$$\frac{\partial}{\partial x} j(x, t) + \frac{\partial}{\partial t} q(x, t) = 0. \quad (39)$$

is obeyed.

The Hamiltonian is written as:

$$\mathcal{H}(t) = \int_0^\ell dx \left[\frac{1}{2C} \left(\frac{\partial\theta}{\partial x} \right)^2 + \frac{L}{2} \left(\frac{\partial\theta}{\partial t} \right)^2 \right] \quad (40)$$

From Hamilton equations of motion, we get the wave equation $\frac{\partial^2\theta}{\partial x^2} - \frac{1}{v^2} \frac{\partial^2\theta}{\partial t^2} = 0$ with velocity $v = 1/\sqrt{LC}$.

The normal mode expansion when the transmission line is considered with stationary boundary conditions at both ends $\theta(0, t) = \theta(\ell, t) = 0$ is given by:

$$\theta(x, t) = \sqrt{\frac{2}{\ell}} \sum_{n=1}^{\infty} b_n(t) \sin k_n x, \quad (41)$$

where $b_n(t)$ is the time-dependent mode amplitude and quantized wavevectors $k_n = \frac{n\pi}{\ell}$. After substitution of this form into the Hamiltonian and integrating over x exploiting orthogonality of the basis functions $[\cos k_n x, \sin k_n x]$ over the interval ℓ gives:

$$\mathcal{H}(t) = \sum_{n=1}^{\infty} \frac{k_n^2}{2C} [b_n(t)]^2 + \frac{L}{2} \left[\frac{db_n(t)}{dt} \right]^2 \quad (42)$$

Quantizing the system in terms of harmonic oscillator ladder operator sets using the correspondence:

$$b_n(t) \rightarrow \sqrt{\frac{\hbar C}{2}} \frac{\sqrt{\omega_n}}{k_n} [a_n^\dagger(t) + a_n(t)] \quad (43)$$

where $\omega_n = \frac{nv\pi}{\ell}$ controls Heisenberg time dependence of ladder operators through $a_n^\dagger(t) = \exp(i\omega_n t) a_n^\dagger(0)$ and $a_n(t) = \exp(-i\omega_n t) a_n(0)$, yields, from charge density $q(x, t) = \frac{\partial\theta(x, t)}{\partial x}$, the voltage at $x = 0$:

$$\begin{aligned} V(t) &= \frac{1}{C} \left[\frac{\partial\theta(x, t)}{\partial x} \right]_{x=0} \\ &= \sqrt{\frac{\hbar}{\ell C}} \sum_{n=1}^{\infty} \sqrt{\omega_n} [e^{i\omega_n t} a_n^\dagger(0) + e^{-i\omega_n t} a_n(0)] \end{aligned} \quad (44)$$

The voltage PSD is obtained after quantum averaging the voltage time correlation (see Appendix A):

$$S_V(\omega) = \frac{2\pi}{\ell C} \sum_{n=1}^{\infty} \hbar\omega_n [n(\omega_n)\delta(\omega+\omega_n) + [n(\omega_n)+1]\delta(\omega-\omega_n)], \quad (45)$$

where $n(\omega) = \langle a_n^\dagger(0)a_n(0) \rangle$ is the photon Bose-Einstein distribution with energy $\hbar\omega$ defined previously as $\langle n \rangle$ in eq. 2.

Taking the limit $\ell \rightarrow \infty$ and converting summation to integration through the replacement

$$\sum_{n=1}^{\infty} f(\omega_n) \approx \frac{\ell}{v\pi} \int_0^{\infty} f(\omega) d\omega \quad (46)$$

yields

$$S_V(\omega) = 2R\hbar\omega \{-n(-\omega)\Upsilon(-\omega) + [n(\omega)+1]\Upsilon(\omega)\}, \quad (47)$$

where $\Upsilon(\omega) = \int_0^{\infty} \delta(\omega-x)dx$ is the Heaviside step function. Physically the negative ω term corresponds to energy absorption whereas in the positive ω case, $n(\omega)$ represents stimulated emission and $+1$ represents spontaneous emission leading to $S_V(\omega)$ being asymmetric with respect to ω in contrast to the classical oscillator case (see Appendix A).

In the $\omega > 0$ case ($\Upsilon(\omega)$ term retained), the spectral density:

$$S_V(\omega) = \frac{2R\hbar\omega}{1 - e^{-\hbar\omega/k_B T}}, \quad (48)$$

reduces, in the classical limit²⁰ $k_B T \gg \hbar\omega$, to Johnson-Nyquist noise result $S_V(\omega) = 2Rk_B T$ (see note¹⁶).

In order to retrieve the quantum fluctuation-dissipation theorem¹⁷, we take the symmetric part of $S_V(\omega)$ by adding positive and negative spectral contributions:

$$S_V(\omega) + S_V(-\omega) = 2R\hbar\omega \coth\left(\frac{\hbar\omega}{2k_B T}\right) \quad (49)$$

IV. APPLICATION TO SECURE COMMUNICATIONS

The main question in this section deals with the possible way to communicate securely with a classical approach based upon acting on communication bits with controlled noise (shift-register generated pseudo-random bits) or through Quantum Communications based on entanglement.

A. Spread spectrum communications

The principle of spread-spectrum communications such as DSSS used in Wi-Fi and cordless telephony is based on multiplying the message (made of 0's and 1's) by a sequence of pseudo-random bits. Pseudo-Random Binary Sequences (PRBS), the digital version of PN sequences are produced in a controlled fashion with a deterministic algorithm akin to pseudo-random numbers used in a Monte-Carlo algorithm or some other type of simulation²⁵.

The main goal of PRBS generation, is to draw 0 or 1 in an equally probable fashion in order to have highly efficient crypting of the message (largest bandwidth or spreading). A particularly efficient method for producing PRBS is based on primitive polynomials modulo 2 or Galois polynomials²⁶ with the following arithmetic:

$$0 \oplus 0 = 0, 0 \oplus 1 = 1, 1 \oplus 0 = 1, 1 \oplus 1 = 0.$$

\oplus is the usual symbol for modulo 2 arithmetic corresponding to the logical XOR operation.

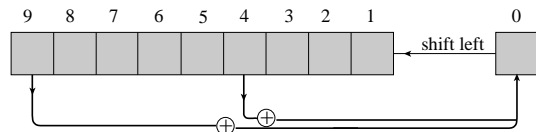


FIG. 3. Shift register connections with feedback set up for PRBS²⁵ generation on the basis of a (modulo 2) primitive polynomial given by $1 + x^4 + x^9$. It is of order 9 and tap connections (9,4,0) are shown.

The coefficients of primitive polynomials modulo 2 are zero or one e.g. $x^4 + x^3 + 1$, moreover they cannot be decomposed into a product of simpler modulo 2 polynomials. An illustrative example is $x^2 + 1$ that cannot be decomposed into simpler polynomials with real coefficients but can be decomposed into polynomials with complex coefficients $x^2 + 1 = (x + i)(x - i)$ with $i = \sqrt{-1}$. When this polynomial is viewed as a Galois polynomial, it is not primitive since it can be decomposed into a product of simpler polynomials $x^2 + 1 \equiv x^2 + 2x + 1 = (x + 1)(x + 1)$ since in modulo 2 arithmetic the term $2x$ is equivalent to 0 according to the above arithmetic rule ($1 \oplus 1 = 0$).

The method for producing PRBS illustrated in fig. 3 requires only a single shift register n bits long and a few XOR or mod 2 bit addition operations (\oplus gates).

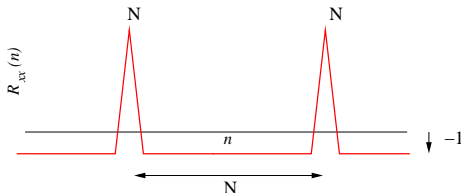
The terms that are allowed to be XOR summed together are indicated by shift register taps. There is precisely one term for each nonzero coefficient in the primitive polynomial except the constant (zero bit) term. Table I contains a list of polynomials for $n \leq 15$, showing that for a primitive polynomial of degree n , the first and last term are 1.

A Maximum-Length Sequence (MLS) $x[n]$ is a balanced sequence made from equally probable symbols with values $+1$ and -1 such that the MLS averages to zero. Choosing $x[n] = (-1)^{a[n]}$ with $a[n] = 0$ or 1 originating from PRBS yields the desired values $x[n] = +1$ or -1 with $+1/-1$ equally probable. The PRBS sequence $a[n]$ is pro-

Connection Nodes	Equivalent Polynomial
(1, 0)	$1 + x$
(2, 1, 0)	$1 + x + x^2$
(3, 1, 0)	$1 + x + x^3$
(4, 1, 0)	$1 + x + x^4$
(5, 2, 0)	$1 + x^2 + x^5$
(6, 1, 0)	$1 + x + x^6$
(7, 1, 0)	$1 + x + x^7$
(8, 4, 3, 2, 0)	$1 + x^2 + x^3 + x^4 + x^8$
(9, 4, 0)	$1 + x^4 + x^9$
(10, 3, 0)	$1 + x^3 + x^{10}$
(11, 2, 0)	$1 + x^2 + x^{11}$
(12, 6, 4, 1, 0)	$1 + x + x^4 + x^6 + x^{12}$
(13, 4, 3, 1, 0)	$1 + x + x^3 + x^4 + x^{13}$
(14, 5, 3, 1, 0)	$1 + x + x^3 + x^5 + x^{14}$
(15, 1, 0)	$1 + x + x^{15}$

TABLE I. List of the first 15 Galois polynomials.

duced with a shift register XOR operation as discussed previously and illustrated in fig. 3. The MLS has many attractive features in addition to the balanced character: its standard deviation and peak values are both equal to 1 making its crest factor (peak/standard deviation) equal to 1, the lowest value it can get²⁵. That is why MLS has noise-immune property²⁵ required in communication electronics. MLS are used not only in secure communications but also in synchronization of digital sequences.

FIG. 4. Property of MLS auto-correlation $R_{xx}[n]$ showing peaks that enables decoding the message and displaying maximum length $N = 2^{n_c} - 1$ with n_c the number of coding bits.

A message $x(t)$ transmitted through a linear time-invariant medium is convoluted with the channel impulse response $h(t)$ resulting in an output message:

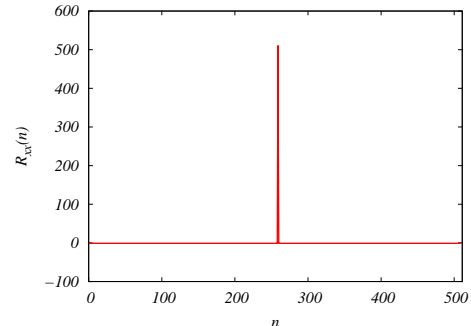
$$y(t) = h(t) * x(t) = \int_{-\infty}^{\infty} h(t-t')x(t')dt' \quad (50)$$

The decoding process of the message is based on a correlation operation based on the $x[n]$ auto-correlation given by:

$$\begin{aligned} R_{xx}[n] &= \frac{1}{N-1} \sum_{i=0}^{N-2} x[i]x[n+i] \\ &= \frac{1}{N-1} \sum_{i=0}^{N-2} (-1)^{(a[i] \oplus a[n+i])} \end{aligned} \quad (51)$$

with $N = 2^{n_c} - 1$ where n_c is the number of coding bits or MLS order. N is the period or the length of the MLS.

As an example, the auto-correlation $R_{xx}[n]$ of order $n_c = 9$ shown in fig. 5 displays a δ function-like behaviour required for message decoding or synchronization (shown in fig. 4).

FIG. 5. Auto-correlation $R_{xx}[n]$ of order 9 MLS displaying the peak value of $2^9-1=511$ over the period interval $[0-511]$.

Another application of the MLS is the determination of the impulse response $h(t)$ of any communication channel by sending through the channel a PRBS signal $x(t)$ whose auto-correlation is a delta function that will be used to identify $h(t)$ at the receiver (see eq. 50) since:

$$h(t) = \int_{-\infty}^{\infty} h(t-t')\delta(t')dt' \quad (52)$$

The impulse response determined with MLS is known to be immune to distortion. This is why despite the fact, many other methods²⁷ exist to measure it with various success, MLS is still preferred when distortion is an issue.

B. Quantum communication (QC)

Quantum Mechanics provides several important ingredients to information communication not present in its classical counterpart²⁸. Firstly the information itself sent across a communication channel can be either classical or quantum. The same applies to the channel that might be classical or quantum. Information transmission is measured with input-output correlations performed across the channel that can also be classical or quantum, the signature of entangled states. Copying a bit in classical communication is a trivial voltage replication operation whereas in QC the no-cloning theorem²⁹ forbids copying quantum information without leaving a trace. Crypting information can be made with classical keys (as in PRBS) or quantum keys. The generation of random numbers through quantum means (QRNG) are superior to PRBS despite their many interesting properties.

Quantum networks across which quantum information is carried is also different from its classical counterpart and finally classical noise as well as quantum noise should

be properly described in order to evaluate information error rates.

We describe every element of quantum communication below.

1. Quantum unit of information: the qubit

The discrete³⁰ unit quantum information in 2D Hilbert space is the qubit, the two-state quantum counterpart of the classical bit (see fig. 6).

It is represented by a two-component wavefunction (or spinor³¹) $|\psi(\theta, \phi)\rangle$.

Computationally, a qubit is representable with 128 classical bits considering that it is made of two complex numbers that are equivalent themselves to four 32 bit (single precision) float numbers.

In the case of photons, quantum states $|0\rangle$ and $|1\rangle$ are equivalent to orthogonal polarization states (see fig. 6).

The photon is the logical choice as the basic information carrier in quantum communications proceeding between nodes that make quantum networks. Information can be encoded in photon polarization, orbital momentum, spatial mode or time and any manipulation targeting processing or information transfer can be made with optical operations, such as using birefringent waveplates to encode polarization...

On the other hand, atoms are the natural choice to make quantum memories since some of their electronic states can retain quantum information for a very long time.

Quantum networks convey quantum information with nodes that allow for its reversible exchange. The latter may be done with two coupled single-atom nodes that communicate via coherent exchange of single photons. In comparison, classical fiber-optic networks use pulses containing typically 10^7 photons each.

In order to prevent change in information or even its loss, it is necessary to have tight control over all quantum network components. Considering the smallest memory for quantum information as a single atom with single photons as message carriers, efficient information transfer between an atom and a photon requires strong interaction between the two components not achievable with atoms in free space but in special optical cavities.

A low-loss cavity made with a set of strongly reflective mirrors alters the distribution of modes with which the atom interacts modifying the density of vacuum fluctuations that it experiences at a given frequency enhancing or reducing atomic radiative properties. As a consequence, spontaneous emission from the atom excited state being a major source of decoherence can be inhibited in a cavity.

A low-loss optical cavity possesses a high quality factor ($Q > 10^3$) allowing a photon entering the cavity to be reflected between mirrors making the cavity several thousand times per second strongly enhancing its coupling with the atom leading to its absorption by the atom

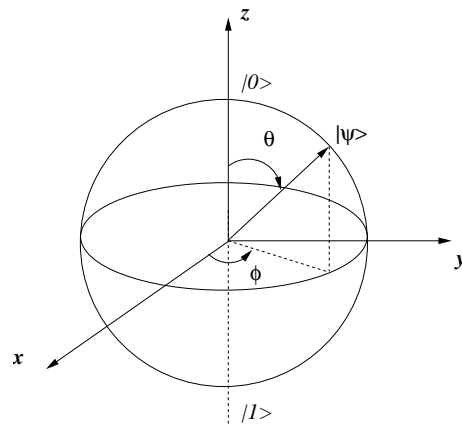


FIG. 6. Bloch sphere (Poincaré sphere for photons) representing the possible values of a quantum information unit in 2D Hilbert space or qubit shown as the quantum wavefunction $|\psi(\theta, \phi)\rangle$. The classical bits (0,1) are the poles of the sphere. A qubit is any two-component wavefunction given by $(\alpha|0\rangle + \beta|1\rangle)$ with complex coefficients α, β . A pure state exists over the Bloch sphere with $|\alpha|^2 + |\beta|^2 = 1$ whereas a mixed state lies inside the sphere with $|\alpha|^2 + |\beta|^2 < 1$. A classical analog³⁰ state lies anywhere on the vertical axis linking the poles.

in a highly efficient coherent fashion.

On the other hand, photon emission by an atom inside a cavity is highly directional and can be sent to other network nodes in a precisely controlled fashion.

Controlling qubit states means that an operator is required to allow switching from one qubit state to another. A rotation matrix $\hat{R}_z(\theta, \phi)$ represents such an operator in the $|0\rangle, |1\rangle$ basis:

$$\hat{R}_z(\theta, \phi) = \begin{bmatrix} \cos \frac{\theta}{2} & -ie^{i\phi} \sin \frac{\theta}{2} \\ -ie^{-i\phi} \sin \frac{\theta}{2} & \cos \frac{\theta}{2} \end{bmatrix} \quad (53)$$

Applying $\hat{R}_z(\theta, \phi)$ on the state $|0\rangle$ allows us to produce an arbitrary state ($\theta \neq 0, \phi \neq 0$) on the Bloch sphere: $|\psi(\theta, \phi)\rangle = \hat{R}_z(\theta, \phi)|0\rangle = \cos \frac{\theta}{2}|0\rangle - ie^{-i\phi} \sin \frac{\theta}{2}|1\rangle \equiv (\alpha|0\rangle + \beta|1\rangle)$. This applies only for pure states that lie on the Bloch sphere surface ($|\alpha|^2 + |\beta|^2 = 1$). In the case of mixed states ($|\alpha|^2 + |\beta|^2 < 1$) we need additional operators that alter also the wavefunction modulus. Experimentally, photon polarization can be rotated with a half-wavelength plate (called also a Hadamard gate), moreover it can be separated into individual components with a polarizing beam-splitter (see ref.³²).

2. Entanglement

Quantum networks possess special features that are not found in their classical counterparts. This is due to the intrinsic nature of the information processed: while a classical bit is either 0 or 1 (see fig. 6), a qubit (quantum bit wavefunction) can take both values at the same

time due to coherent superposition inherent to Quantum Mechanics linearity.

Quantum Mechanics embodies the notion of entanglement detected with violation of Bell inequalities⁹ and that brings a paradigm shift into information processing.

Given two qubits $|Q_1\rangle = \frac{1}{\sqrt{2}}(c_0|0\rangle + c_1|1\rangle)$ and $|Q_2\rangle = \frac{1}{\sqrt{2}}(d_0|0\rangle + d_1|1\rangle)$, it is possible to build a state $|Q_1, Q_2\rangle = |Q_1\rangle \otimes |Q_2\rangle$ such that:

$$\begin{aligned} |Q_1, Q_2\rangle &= \frac{1}{\sqrt{4}}(c_0|0\rangle + c_1|1\rangle) \otimes (d_0|0\rangle + d_1|1\rangle) \\ &= \frac{1}{\sqrt{4}}(c_0d_0|0,0\rangle + c_0d_1|0,1\rangle + c_1d_0|1,0\rangle + c_1d_1|1,1\rangle) \end{aligned} \quad (54)$$

Quantum Mechanics, however, allows for building other states such as: $|Q\rangle = \frac{1}{\sqrt{2}}(c_0d_1|0,1\rangle + c_1d_0|1,0\rangle)$ which are not decomposable into products of constituent states.

These states are called entangled and can be mapped onto the polarization of single photons which can be transferred through an optical fiber between two nodes consisting respectively of atoms in state $|A\rangle$ and state $|B\rangle$.

Quantum mechanical entanglement ought to be achieved between the two nodes in order to have successful QC maintained over the coherence time preserving integrity of quantum information transfer.

In order to achieve entanglement between two remote network nodes, polarization of the single photon emitted by atom in state $|A\rangle$ is entangled with the atomic quantum state.

Once the photon gets absorbed, the entanglement is transferred onto atom in state $|B\rangle$ and reversible exchange of quantum information is performed between the two nodes.

Experimental production of entanglement can be made between two particles (bipartite) or between several particles (multipartite) and for each number of particle (two, three, four ...) case or particle type (atoms, electrons, photons...) several experimental procedures readily exist. It is not limited to microscopic particles since it can be induced by a light pulse between two macroscopic objects³³ consisting each of a gas containing about 10^{12} Cesium atoms.

Entanglement can occur when particles interact and kept in contact or when they emerge from a common ancestor as in the EPR⁷ case where a spinless particle decays into two particles carrying opposite spins... Another example is the case of a photon interacting with a non-linear crystal. It can be destroyed and replaced with a lower energy entangled photon pair (the process is called SPDC³⁴ or Spontaneous Parametric Down-Conversion).

Heralded³⁵ entanglement may occur between non-interacting remote particles (Yb ions held in two ion traps, 1 meter apart) not possessing a common ancestor, however the entanglement probability p_E is very low

($p_E \approx 10^{-9}$) since entanglement results from the interaction of decay photons emitted by each ion after their excitation by picosecond laser pulses. Thus p_E needs to be increased substantially in order to make it applicable to mass QC.

3. Quantum Random Number Generation

Classical Random Number Generators (RNG) are based on Uniform RNG and the standard statistical quality tests target the uniformity²⁵ of the numbers generated. Quantum Mechanics introduce a predictability test to further improve quality of RNG.

This means that even if the RN is perfectly uniformly distributed, it may contain hidden deterministic information and is therefore prone to be predictable. For instance, PN and PRBS generate uniformly distributed numbers but since they are produced with a deterministic algorithm, an eavesdropper might, by drawing values and performing statistical analysis²⁵, be able to make an educated guess and access the cipher password, key...

Thus, statistical uniformity tests are necessary but not sufficient to guarantee that any given RNG is not prone to attack and guess by an intruder. Quantum RNG (QRNG) offers "true RN" generation that is very difficult to predict. Using a special program called "randomness extractor"³⁶ one might eliminate all bit strings originating from an implicit deterministic algorithm and keep only truly random bit strings. For this reason, the method is also called, amplification of weak randomness³⁶.

Randomness extraction procedure exploits entropy hierarchy (see Appendix D) that attributes a number of bits depending on the entropy estimation used. Rényi min-entropy is very efficient computationally wise and a string of perfectly random bits has unit min-entropy per bit as derived in Appendix D.

Starting from l input bits X_i of low-entropy per bit ($s < 1$), the extractor computes a number $k < l$ of higher-entropy ($s' \approx 1$) output bits Y_j with a linear transformation via multiplication by a matrix m :

$$Y_j = \sum_{i=1}^l m_{ji} X_i, \quad j = 1 \dots k \quad (55)$$

m is built from $l \times k$ random bits that can be generated with Galois polynomials and all arithmetic operations are done modulo 2 with AND and XOR logic.

This "Whitening" procedure can be viewed as the quantum counterpart of the Maximum Entropy Method that is widely used in Image Processing for deblurring images²⁵.

As a direct application of this concept, Sanguinetti *et al.*³⁷ used Smartphone cameras to produce Quantum Random Numbers. After uniform illumination of the camera image sensor by a LED and estimation of the number of photons generated per pixel, a randomness

extractor algorithm such the above (eq. 55) is used to compute truly random numbers.

For X_i input bits with low entropy per bit ($s < 1$), the probability that the output Y_j deviates from a perfectly random bit string (with high entropy per bit $s' \approx 1$) is bounded³⁸ by:

$$\epsilon = 2^{-(ls - ks')/2}, \quad (56)$$

Picking a CCD image sensor with 16 bits per pixel (detection capability) and a photon flux producing 2×10^4 electrons per pixel gives $R_\infty = 8.469$ bits/pixel (from eq. D7) yielding a min-entropy per bit $s = 0.529$ (in comparison, Shannon Entropy is 9.191 bits/pixel or 0.574 per bit). Selecting input $l = 2000$, output $k = 400$ and $s' = 1$, we get $\epsilon = 2.57 \times 10^{-197}$.

As a result, an eavesdropper would have to generate an extremely large³⁸ amount of random numbers (about 1.97×10^{99}) before noticing any departure from a perfectly random sequence, indicating the superior performance of QRNG with respect to any classical RNG.

4. Quantum Keys

Classical cryptography is based on two types of keys that are used to encode and decode messages: secret or symmetric keys and public or asymmetric keys. Symmetric keys are same for encoding and decoding messages whereas in public cryptography systems, one needs a public key and a private key. In the PGP (Pretty Good Privacy) secure mailing system over the Internet, the sender encodes the message with receiver public key and the receiver decodes the message with his private key. In quantum cryptography, the simplest example of secret key sharing among sender and receiver (Alice and Bob) in QKD is the BB84²⁹ protocol. Alice and Bob communicate through two channels: one quantum to send polarized single photons and one classical to send ordinary messages. Alice selects two bases in 2D Hilbert space consisting each of two orthogonal states: \oplus basis with $(0, \pi/2)$ linearly polarized photons, and \otimes basis with $(\pi/4, -\pi/4)$ linearly polarized photons.

Four symbols: $|\rightarrow\rangle, |\uparrow\rangle, |\nearrow\rangle, |\searrow\rangle$ representing polarized single photons are used to transmit quantum data with $|\nearrow\rangle = \frac{1}{\sqrt{2}}(|\rightarrow\rangle + |\uparrow\rangle)$ and $|\searrow\rangle = \frac{1}{\sqrt{2}}(|\rightarrow\rangle - |\uparrow\rangle)$.

In the *(basis, data)* representation, the symbols are given by $|\rightarrow\rangle = (\oplus, 0)$, $|\uparrow\rangle = (\oplus, 1)$ in the \oplus basis whereas $|\searrow\rangle = (\otimes, 0)$, $|\nearrow\rangle = (\otimes, 1)$ in the \otimes basis.

A message transmitted by Alice to Bob over the Quantum channel is a stream of symbols selected randomly among the four described above.

Bob performs polarization measurements over the received symbols selecting randomly bases \oplus or \otimes .

Afterwards Bob and Alice exchange via the classical channel their mutual choice of bases without revealing the measurement results.

In the ideal case (no transmission errors, no eavesdropping) Alice and Bob should discard results pertaining to

measurements done in different bases (or when Bob failed to detect any photon). This process is called "key sifting" after which the raw key is determined.

After key sifting, another process called key distillation²⁹ must be performed. This process entails three steps²⁹: error correction, privacy amplification and authentication in order to reveal classical or quantum errors of transmission, detect eavesdropping (with the no-cloning theorem²⁹) and act against it.

Ignoring, for simplicity, key distillation, the raw key size is typically about one quarter of the data sent since both Alice and Bob are selecting their bases at random (total probability is roughly $\frac{1}{2} \times \frac{1}{2} = \frac{1}{4}$).

A random number generator (RNG) or rather a random bit generator can be used to select \oplus or \otimes bases. Using PRBS or, even better, QRNG to select measurement bases, we infer that by comparison with the classical FHSS crypting method, Quantum Mechanics provides extra flexibility through basis selection. Such option is simply not available in classical communication.

On the negative side, there are several problems that may come up with the BB84 scheme. One major obstacle is that presently, it is difficult, on a large scale level, to produce single photons. One approximate method for doing this, is to use attenuated laser pulses containing several photons that might be intercepted in the quantum channel by an eavesdropper with a PNS (Photon Number Splitting) attack.

Quantum Communications can be made more secure when QKD is implemented with entanglement²⁹ providing a secure way to distribute secret keys between remote users such that when some eavesdropper is detected, the transmission is halted and the data discarded.

The BBM92²⁹ scheme is an entanglement based version of the BB84 protocol. Polarization entangled photon pairs (called EPR pairs or Bell states) are sequentially generated with one photon polarization measured by Alice and the other measured by Bob. EPR pairs are produced after emerging from SPDC⁷ by using a birefringent phase shifter or slightly rotating the non-linear crystal itself since the state produced by SPDC is:

$$|\psi\rangle = \frac{1}{\sqrt{2}}(|\rightarrow\uparrow\rangle + e^{i\varphi} |\uparrow\rightarrow\rangle) \quad (57)$$

Thus it suffices to modify φ to 0 or π or place a quarter wave-plate giving a 90° shift in one photon path to generate all Bell states³⁴. These states are polarization entangled²⁹ photons :

$$|\psi^\pm\rangle = \frac{1}{\sqrt{2}}(|\rightarrow\uparrow\rangle \pm |\uparrow\rightarrow\rangle), |\phi^\pm\rangle = \frac{1}{\sqrt{2}}(|\rightarrow\rightarrow\rangle \pm |\uparrow\uparrow\rangle) \quad (58)$$

The set forms a complete orthonormal basis in 4D Hilbert space for all polarization states of a two-photon system.

Alice and Bob choose randomly one of the two bases \oplus or \otimes to perform photon polarization measurement.

Afterwards Alice and Bob communicate over the classical channel which basis they used for each photon successfully received by Bob.

The raw key is obtained by retaining the results obtained when the bases used are same. Neither RNG nor QRNG are used in this case since randomness is inherent to the EPR pair polarization measurement²⁹. Moreover, no Bell inequality tests are needed since all measurements must be perfectly correlated or anti-correlated.

For instance in the $|\psi^+\rangle$ state, if one photon is measured to be in the $|\rightarrow\rangle$ state, the other must be in the $|\uparrow\rangle$ since the probabilities of measuring $\rightarrow\rightarrow$ or $\uparrow\uparrow$ are given by $|\langle\rightarrow\rightarrow|\psi^+\rangle|^2 = |\langle\uparrow\uparrow|\psi^+\rangle|^2 = 0$, whereas the probabilities of measuring $\rightarrow\uparrow$ and $\uparrow\rightarrow$ are $|\langle\rightarrow\uparrow|\psi^+\rangle|^2 = |\langle\uparrow\rightarrow|\psi^+\rangle|^2 = \frac{1}{2}$. This is termed perfect anti-correlation.

When the polarization measurements are performed in the \otimes basis, we get rather, perfect correlation. That means the probabilities of measuring $\nearrow\nrightarrow$ or $\searrow\swarrow$ are $|\langle\nearrow\nrightarrow|\psi^+\rangle|^2 = |\langle\searrow\swarrow|\psi^+\rangle|^2 = 0$, whereas the probabilities of measuring $\nearrow\swarrow$ or $\searrow\nrightarrow$ are given by $|\langle\nearrow\swarrow|\psi^+\rangle|^2 = |\langle\searrow\nrightarrow|\psi^+\rangle|^2 = \frac{1}{2}$.

Note that if we rather consider the $|\psi^-\rangle$ state, we get perfect anti-correlation in both bases \oplus and \otimes .

5. Quantum Networks

In classical communications, channel transfer function, the Fourier transform of its impulse response $h(t)$ is a function of frequency and distance. Channel bandwidth and signal attenuation are functions of distance. When a pulse (representing a communication symbol made of several bits depending on the modulation method used) is sent through an optical fiber, it undergoes broadening leading to inter-symbol interference, attenuation leading to signal loss and alteration due to noise. Thus it is required to evaluate the largest distance that could be covered at the end of which a repeater is placed in order to filter out noise and restore pulse shape to its original form.

In QKD, Alice and Bob should be able to determine efficiently their shared secret key as a function of distance L separating them. Since, the secure key is determined after sifting and distillation, secure key rate is expressed in bps (bits per symbol) given that Alice sends symbols to Bob to sift and distill with the remaining bits making the secret key.

The simplest phenomenological way to estimate secure key rate versus distance $K(L)$ is to consider a point-to-point scenario with $K(L) \propto [A(L)]^n$ where $A(L) = 10^{-\alpha_0 L/10}$ is signal attenuation versus distance. α_0 is the attenuation coefficient per fiber length and $n = 1, 2, \dots$. α_0 depends strongly on the wavelength λ used to transmit information through the fiber. For the standard Telecom wavelength¹ $\lambda = 1.55\mu\text{m}$, $\alpha_0 = 0.2$ dB/km.

The optimal distance²⁹ L_{opt} is determined by the maximum of the objective function $LK(L)$. Taking the deriva-

tive and solving, we get $L_{opt} = \frac{10}{n\alpha_0 \ln(10)}$.

This yields $L_{opt} = 21.7$ kms for $n = 1$, $L_{opt} = 10.86$ kms for $n = 2$ and $L_{opt} = 5.43$ kms for $n = 4$.

Errors produced by noise, interference and damping are represented by a *BER* (Bit Error Rate), the ratio of wrong bits over total number of transmitted bits. *BER* versus distance is an important indicator of communication quality as much as communication speed is represented by bit rate versus distance.

In the quantum case, the *QBER* (Quantum *BER*) $Q_e(L)$ versus distance is the quantity of interest. Regarding the BB84 protocol case, a simple model³⁹ delivers the expression:

$$Q_e(L) = \frac{P_e}{A(L)\mu\eta_{Bob} + 2P_e} \quad (59)$$

where P_e is the probability of error per clock cycle (measured to be 8.5×10^{-7}). $\mu = 0.1$ is the average photon flux used by Alice to transmit symbols and $\eta_{Bob} = 0.045$ is Bob apparatus detection efficiency. The results are displayed versus distance L in fig.7.

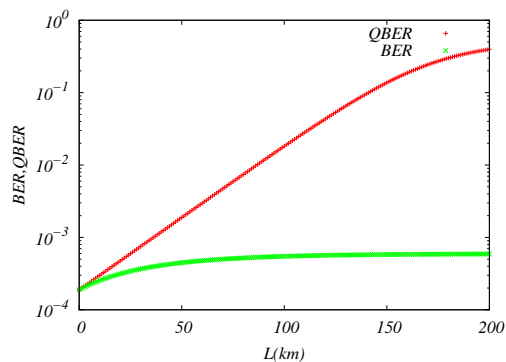


FIG. 7. (Color on-line) Classical *BER* and quantum *QBER* versus distance L along an optical fiber using the BB84 protocol considering they start from the same value at $L = 0$.

Fig. 7 shows that the *QBER* increases faster and takes larger values than the optical fiber classical *BER*. For many digital lightwave systems using ON-OFF modulation¹ (1 for light pulse, 0 for no pulse), the classical *BER* is typically about 10^{-9} and may reach values in the $[10^{-16} - 10^{-15}]$ range.

Moving on to estimate the secure key generation rate in bits per symbol (bps) emitted by Alice, a simple model for the BB84 protocol⁴⁰ gives:

$$K(L) = G_\mu \{-h_2(Q_e(L)) + \Omega[1 - h_2(e_1)]\} \quad (60)$$

where G_μ is the gain for an average photon flux μ . Ω is the fraction of events detected by Bob and produced by single-photon signals emitted by Alice. e_1 is the corresponding *QBER* and h_2 is the binary Shannon entropy¹

given by $h_2(x) = -x \log_2(x) - (1-x) \log_2(1-x)$. Using the same parameters as in Ref.³⁹ and bounds for Ω and e_1 estimated in Ref.⁴⁰, we are able to plot the secure key rate versus distance for several values of the detector error rate e_D as displayed in fig. 8.

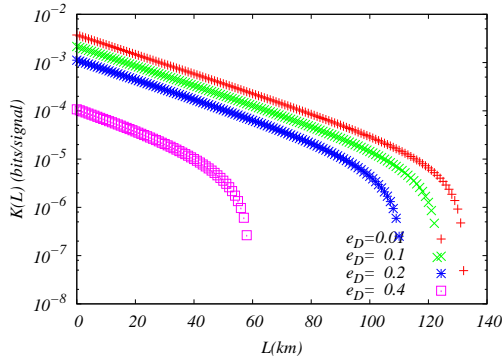


FIG. 8. (Color on-line) Key rate $K(L)$ in bps versus distance L using the same parameters as in Ref.⁴⁰ for several detector error rates $e_D=0.01, 0.1, 0.2$ and 0.4 .

Fig. 8 shows that the key rate is small and given that security increases with key length, a major improvement with respect to this simple approach should be undertaken in order to increase substantially the bps rate.

Recently, a joint team from Cambridge Science Park and University of Cambridge⁴¹ succeeded to increase substantially the secure key rate using detectors operating at room temperature. The secure key rates obtained were between 1.79 Mbit/s and 1.2 kbit/s for fiber lengths between 40 km and 100 km, respectively.

Regarding network building developments, the first elementary quantum network based on interfaces between single atoms and photons located at two network nodes installed in two distant laboratories connected by an optical fiber link was made in 2012 by a team of scientists⁴² at the Garching MPQ.

Using the above procedures, Ritter *et al.*⁴² were able to generate entanglement between two remote nodes in two different laboratories separated by a distance of 21 meters and linked by an optical fiber. They were able to maintain entanglement for about 100 microseconds while entanglement generation itself took about a single microsecond.

Later, a team from Technical University of Vienna⁴³ succeeded in coupling Cesium atoms to an optical fiber and storing quantum information over a period of time that is long enough to sustain entanglement over distances (hundreds of kilometers) that are large enough to achieve reliable long distance communication.

The Vienna team extended coherence time to several milliseconds and given that speed of light in an optical fiber is about 200 kilometers per millisecond, a substantial separation increase is henceforth achievable potentially reaching several hundred kilometers between nodes

over which entanglement and coherence are maintained, paving the way to long-distance QC.

6. Quantum noise

At low temperature, very high frequency $hf > k_B T$, mesoscopic scale or when considering single carrier, quantum dot devices... quantum noise becomes larger than thermal implying a full reconsideration of traditional electronics that has long been described by White (thermal noise with no relaxation time), Shot noise based on a single relaxation time (such as generation-recombination noise in semiconductors), Pink noise ($1/f$) originating from a distribution of relaxation times...

Recently, entanglement has been shown to appear spontaneously in photon-assisted electrical noise occurring in quantum conductors consisting of an ac-biased tunnel junction cooled at low temperature⁴⁴.

The experiments were performed in Sherbrooke⁴⁴ at 18 mK⁴⁵ on a Al/Al₂O₃/Al tunnel junction with resistance of 70 Ω , the signal being emitted by the junction analyzed at two frequencies $f_1=7$ GHz and $f_2=7.5$ GHz.

The total voltage applied on the junction is given by $V_{dc} + V_{ac} \cos 2\pi f_0 t$ with frequency $f_0 = f_1 + f_2$ chosen to produce optimal junction response as explained below.

Firstly, junction noise becomes photon-assisted because ac-biasing injects photons in the junction.

Secondly, statistical correlations between currents at f_1 and f_2 as a function of dc voltage showed that photons generated in pairs in the junction are entangled since their correlations violate Bell inequalities⁹ as discussed below. Defining "position" X_1, X_2 and "momentum" operators P_1, P_2 from frequency dependent current operators $I(\pm f_1), I(\pm f_2)$ as:

$$X_{1,2} = \frac{I(f_{1,2}) + I(-f_{1,2})}{\sqrt{2}}, P_{1,2} = \frac{I(f_{1,2}) - I(-f_{1,2})}{i\sqrt{2}} \quad (61)$$

we use the QFDT (see section III) to evaluate the various quantum correlations versus dc voltage V_{dc} applied to the Al/Al₂O₃/Al tunnel junction for a fixed ac voltage $V_{ac}=37 \mu\text{V}$ in fig. 9. Violation of Bell inequalities displayed by $\langle X_1 X_2 \rangle$ and $\langle P_1 P_2 \rangle$ for non-zero V_{ac} indicate entanglement in contrast with the other correlators that do not display any variation with V_{dc} . $\langle X_1 X_2 \rangle_0$ and $\langle P_1 P_2 \rangle_0$ that are evaluated for $V_{ac} = 0$ do not show violation of Bell inequalities indicating that it is V_{ac} that induces quantum correlations thus yielding a simple electrical control parameter for entanglement.

V. DISCUSSIONS AND CONCLUSIONS

In this work, the main unifying thread for the description of fluctuations, noise and noise-based communication is the ubiquitous presence of harmonic oscillators represented mostly by photons.

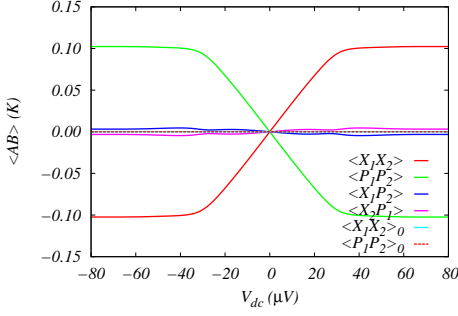


FIG. 9. (Color on-line) Correlations in Kelvin units between currents at frequencies f_1 and f_2 versus V_{dc} voltage applied to the Al/Al₂O₃/Al tunnel junction for a fixed ac voltage $V_{ac} = 37 \mu\text{V}$. Violation of Bell inequalities is displayed only by $\langle X_1 X_2 \rangle$ and $\langle P_1 P_2 \rangle$ quantum correlations for non-zero applied ac voltage whereas all other correlators are null including $\langle X_1 X_2 \rangle_0$ and $\langle P_1 P_2 \rangle_0$ that are evaluated when the ac voltage is zero.

While secure classical noise-based communication uses spread-spectrum sequences, secure QC based on QKD implemented with entanglement ties communicating parties in a way such that any attempt by some eavesdropper to intercept or interfere in the communication process is immediately sensed and treated appropriately.

Entanglement may be done between quantum objects such as atoms, electrons, photons etc... however the preferred information carrier is the photon and the entanglement that can be based on polarization, momentum, spatial mode or time can be sustained over very large distances as demonstrated by the Vienna experiment.

Heralded entanglement not necessitating a common ancestor has even been applied by the same Garching⁴⁶ (MPQ) group to transfer a polarization qubit from a photon to a single atom with 39% efficiency and perform the reverse process, that is from the atom to a given photon with an efficiency of 69%, proving once again that a long-distance QC network based on entangled photons is a serious contender for secure communication.

On the other hand, the Sherbrooke experiment shows that a major component of noise-based QC is built within quantum noise since entanglement is produced in quantum conductors by a simple electrical (ac voltage) control.

Even if presently such entanglement occurs at very low temperature (18 mK), the result is still important since that particular type of entanglement could be exploited after appropriate conditioning with quantum cryptography techniques in order to secure information transfer and communication.

Presently several secure QC schemes not based on entanglement exist, moreover some other protocols not relying on key generation and distribution have also been developed.

For instance QSDC (Quantum Secure Direct Communication) is a branch of QC in which the message is sent directly between remote users without generating a key to encrypt it.

Practicality and robustness of schemes used in QC for securing transmission of information will finally decide which of the different methods and protocols will be ultimately adopted as reliable for secure mass communication.

Appendix A: Stochastic processes and Noise

A stochastic process is a random function of time that behaves in a way such that every value ξ it takes is distributed with a PDF $p(\xi; t)$:

$$\langle \xi(t) \rangle = \int_{-\infty}^{\infty} \xi p(\xi; t) d\xi \quad (\text{A1})$$

The ensemble¹⁵ average $\langle \dots \rangle$ is taken over the possible occurrences of the random function $\xi(t)$.

When the PDF is given by a Boltzmann distribution as illustrated in Section II, the ensemble average is called thermal:

$$\langle \xi(t) \rangle_{\beta} = A \int_{-\infty}^{\infty} \xi e^{-\beta E} d\xi \quad (\text{A2})$$

with A a normalization constant, E the system energy and β the inverse temperature.

Time average of $\xi(t)$ is defined by:

$$\overline{\xi(t)} = \lim_{T \rightarrow +\infty} \frac{1}{T} \int_0^T \xi(t) dt \quad (\text{A3})$$

In this work we assume the validity of the Ergodic theorem^{15,47} that ensures the equivalence of time averaging and ensemble averaging.

The ensemble average of the random function $\xi^2(t)$ is given by:

$$\langle \xi^2(t) \rangle = \int_{-\infty}^{\infty} \xi^2 p(\xi; t) d\xi \quad (\text{A4})$$

whereas the mean-squared ensemble average is given by $\langle \delta \xi^2 \rangle = \langle \xi^2(t) \rangle - \langle \xi(t) \rangle^2$. The auto-correlation depending on two instants t_1, t_2 is:

$$\mathcal{R}(t_1, t_2) = \langle \xi(t_1) \xi(t_2) \rangle = \int_{-\infty}^{\infty} \int_{-\infty}^{\infty} \xi_1 \xi_2 p(\xi_1, \xi_2; t_1, t_2) d\xi_1 d\xi_2 \quad (\text{A5})$$

with $p(\xi_1, \xi_2; t_1, t_2)$ representing the two times PDF for the distribution of the variables ξ_1, ξ_2 .

Note that in the quantum case, ensemble average is replaced by quantum average.

For a stationary process we have the properties: $\langle \xi(t) \rangle = \text{constant}$, and $\mathcal{R}(t_1, t_2) = R(t_1 - t_2)$, with R a function of a single argument in contrast with \mathcal{R} .

Taking $t_1 = t$ and $t_2 = t + \tau$ we infer that $\mathcal{R}(t, t + \tau) = R(\tau)$ is a function of τ only meaning it is independent of the instant t at which we start observing the process and depends only of the interval of time τ during which it is being observed.

Actually we have a symmetry under the exchange of the time instants t_1, t_2 resulting into the property:

$$\mathcal{R}(t_1, t_2) = \mathcal{R}(t_2, t_1) = R(|t_1 - t_2|) \quad (\text{A6})$$

Moreover, we expect physically decorrelation of the variables t_1, t_2 as the delay separating them increases, that is: $R(|t_1 - t_2|)$ is a decreasing function of its argument $|t_1 - t_2|$.

The Ergodic theorem¹² specifies that ensemble average is equivalent to time average in many systems. In glassy systems, ergodicity is not valid.

Stationary noise like any other stochastic process has an auto-correlation function $\mathcal{R}(t, t + \tau)$ function of only τ , hence we can use the definition $R(\tau) = \mathcal{R}(t, t + \tau) = \mathcal{R}(0, \tau)$.

This leads to classifying noise according to its Power Spectral Density (PSD) defined as the Fourier transform of the auto-correlation function $R(\tau) = \langle V(t)V(t + \tau) \rangle$ of the voltage fluctuations:

$$S_V(f) = \int_{-\infty}^{+\infty} \exp(-i2\pi f\tau) R(\tau) d\tau \quad (\text{A7})$$

Note that the integral prefactor is 1 whereas in the angular frequency case $S_V(\omega)$, the prefactor is 2π . The inverse Fourier transform yields:

$$R(\tau) = \int_{-\infty}^{+\infty} \exp(i2\pi f\tau) S_V(f) df \quad (\text{A8})$$

The validity of the direct and inverse Fourier transforms is conditioned by the existence of the respective integrals:

$$\int_{-\infty}^{+\infty} |R(\tau)| d\tau < \infty, \quad \int_{-\infty}^{+\infty} |S_V(f)| df < \infty \quad (\text{A9})$$

When $\tau = 0$ we get $\langle V(t)V(t) \rangle = R(0) = \int_{-\infty}^{+\infty} S_V(f) df$.

In the case of classical systems, the auto-correlation is always real and thus the PSD is always symmetric with respect to the frequency. Consequently it is possible to rewrite the above formulae as:

$$S_V(f) = 4 \int_0^{+\infty} \cos(2\pi f\tau) R(\tau) d\tau, \\ R(\tau) = \int_0^{+\infty} \cos(2\pi f\tau) S_V(f) df \quad (\text{A10})$$

The auto-correlation may also be written as $R(\tau) = \langle V(\tau)V(0) \rangle - \langle V \rangle^2$. A simple classification of Noise is possible when the PSD behaves approximately as $S(f) \sim 1/f^n$. Consequently we have the following cases:

- Blue noise: $n = -1$ or $S_V(f) \sim f$. This originates from the blue glow observed in Cherenkov radiation emitted by a charged particle traveling in a dielectric at a velocity larger than light phase velocity in that medium.
- White noise: $n = 0$ or $S_V(f) \sim \text{constant}$. This is noise heard when a radio or TV broadcast station has stopped emitting.
- Pink noise: $n = 1$ or $S_V(f) \sim 1/f$. $1/f$ noise is encountered in many areas of Science and Technology. It is called also flicker noise and occurs also in music, earthquakes, floods...
- Brown noise: $n = 2$ or $S_V(f) \sim 1/f^2$. This is analogous to random walk (Brownian motion) and the PSD falls faster than $1/f$.
- Black noise: $n > 2$ or $S_V(f) \sim 1/f^n$. This is the opposite of white noise, in the sense that the PSD falls off very quickly.

Appendix B: The classical fluctuation-dissipation theorem (FDT)

Einstein developed in 1905 a theory that explained Brownian motion on the basis of the kinetic theory of gases.

The 1D motion of the particle is essentially a random walk, with steps to right and left as equally probable.

Einstein suggested that the mean kinetic energy per degree of freedom of the particle should be given by statistical mechanics and the equipartition of energy as:

$$\frac{1}{2} m \langle v^2 \rangle = \frac{1}{2} k_B T \quad (\text{B1})$$

where m is the mass of the particle, v its instantaneous velocity component in the x -direction, the mean-squared value $\langle v^2 \rangle$ is equal to the time average $\langle v^2 \rangle$ and Einstein did not make a distinction between the two averages assuming Ergodicity.

The displacement x in the x -direction during the time interval t . Einstein showed that

$$\langle (x - \langle x \rangle)^2 \rangle = 2Dt \quad (\text{B2})$$

with D the diffusion constant of the particle.

Let us prove these results directly from a classical equation of motion extended to comprise random excitation terms (Langevin equation):

$$m \frac{dv(t)}{dt} = -\alpha v + \xi(t) \quad (\text{B3})$$

The viscous term αv with coefficient $\alpha = 6\pi\eta a$ is a Stokes term depending on an average damping coefficient η on the particle from irregular impacts on the particle with radius a from the surrounding fluid.

$\xi(t)$ is a random term originating from the surrounding medium considered as a reservoir at temperature T with the following statistical properties:

$$\langle \xi(t) \rangle = 0 \text{ and } \langle \xi(t)\xi(t') \rangle = \lambda\delta(t-t') \quad (\text{B4})$$

The above Langevin equation¹⁵ contains a time-dependent random excitation term $\xi(t)$ in an otherwise ordinary differential equation (ODE) (see Section II).

Writing $\alpha = m\gamma$ we perform a direct integration of the first-order ODE:

$$v(t) = v_0 e^{-\gamma t} + \frac{1}{m} \int_0^t \xi(t') e^{-\gamma(t-t')} dt' \quad (\text{B5})$$

with v_0 the initial velocity at $t = 0$. The average of eq. 18 yields $\langle v(t) \rangle = v_0 e^{-\gamma t}$ since $\langle \xi(t) \rangle = 0$. This indicates that γ is an inverse relaxation time of the initial velocity much like $1/RC$ in the circuit encountered in Section II.

The auto-correlation of the velocity is given by:

$$\sigma_v^2(t) = \langle v(t)v(t') \rangle - \langle v(t) \rangle \langle v(t') \rangle = \frac{\lambda}{m^2} \exp(-\gamma|t-t'|) \quad (\text{B6})$$

In order to get the value of λ we recall Einstein (asymptotic) result of Brownian motion.

Setting $t = t'$ and identifying $\frac{\lambda}{m^2}$ with $\frac{D}{\gamma}$ we get the value of λ . Thus:

$$\sigma_v^2(t) = 2D \int_0^t \xi(t') e^{-2\gamma(t-t')} dt' = \frac{D}{\gamma} (1 - e^{-2\gamma t}), \quad t > 0 \quad (\text{B7})$$

This means velocity dispersion increases initially with time $\sigma_v^2(t) = 2Dt$ when time $t \ll \tau_r$, to finally saturate at the value $\sigma_v^2(t) \sim \frac{D}{\gamma}$ for time $t \gg \tau_r$.

Taking account of the average kinetic energy $\langle E \rangle = m \langle v(t)^2 \rangle / 2$ and recalling the equipartition theorem $\langle E \rangle = k_B T / 2$, we get $\gamma = \frac{m}{k_B T} D$.

Hence we can rewrite the auto-correlation formula as:

$$\gamma = \frac{1}{2mk_B T} \int_{-\infty}^{\infty} \langle \xi(t)\xi(t+\tau) \rangle d\tau \quad t > 0 \quad (\text{B8})$$

This is the classical fluctuation-dissipation theorem with auto-correlation representing fluctuation and friction coefficient γ representing dissipation.

Appendix C: Density of states for particles and elementary excitations

According to Kittel⁴⁸ the density of states of solid-state excitations $g(\omega)$ in d dimensions for a system of typical linear length ℓ is given by $g(\omega) = \left(\frac{\ell}{2\pi}\right)^d \int \frac{dS_\omega}{v_g}$ with \mathbf{k} integration performed such that $\omega < \omega(\mathbf{k}) < \omega + d\omega$. $\epsilon(\mathbf{k}) = \hbar\omega(\mathbf{k})$ is the energy dispersion, v_g is the group velocity modulus of the elementary excitations⁴⁸: $v_g = \frac{1}{\hbar} |\nabla_{\mathbf{k}} \epsilon(\mathbf{k})|$ and dS_ω is the differential area element on the constant energy surface $\omega(\mathbf{k}) = \omega$. It is possible to generalize this formula to $g(\omega) = N_p \left(\frac{\ell}{2\pi}\right)^d \int \frac{dS_\omega}{v_g}$ where N_p is the number of excitation polarizations.

When the excitations are real particles (photons, electrons...) and possess a spin S , $N_p = 2S + 1$ when the particles have non-zero mass (electrons) and $N_p = 2$ for zero-mass particles (such as photons). E. Wigner⁴⁹ showed in 1939, on the basis of Lorentz invariance, that the photon (or any other massless particle with spin S) moves with the velocity of light c , even in the center-of-mass frame. Exploiting rotational symmetry around c direction yields only two polarizations: left or right circular corresponding to $m_S = \pm S$ spin eigenstates.

In the case of elementary excitations (phonons, plasmons, magnons, excitons...) $N_p = 1$ regardless of the statistics.

Specializing to the "Debye" case $\omega(\mathbf{k}) = v_g |\mathbf{k}| = v_g k$, the above expression of the density of the states can be expressed analytically since the constant energy surface $\omega(\mathbf{k}) = \omega$ is a hypersphere with radius $k = \omega/v_g$ and surface equal to $S_\omega = s_1 k^{d-1}$ where s_1 is the unity radius hypersphere surface given by¹² $s_1 = 2\pi^{d/2} / \Gamma(d/2)$.

Collecting expressions we get $g(\omega) = N_p \left(\frac{\ell}{2\pi}\right)^d \frac{S_\omega}{v_g}$ thus

$$g(\omega) = N_p \left(\frac{\ell}{2\pi}\right)^d \frac{1}{v_g} \frac{2\pi^{d/2}}{\Gamma(d/2)} \left(\frac{\omega}{v_g}\right)^{d-1}$$

In an oscillator, excitations are quantized with average energy for n quanta as $\hbar\omega(\langle n \rangle + \frac{1}{2})$ in the interval $[\omega, \omega + d\omega]$. Multiplying the mean energy by the number of quanta (modes) $g(\omega)d\omega$ in this interval yields: $g(\omega)\hbar\omega(\langle n \rangle + \frac{1}{2})d\omega$.

Appendix D: Entropy hierarchy

In order to establish a hierarchy of information entropies, recall that Shannon entropy is defined (in the

discrete probability case) by:

$$H_S = - \sum_{i=1}^N p_i \log_2 p_i \quad (\text{D1})$$

with p_i the probability of occurrence of symbol i and N the total number of symbols.

Guided by Hamming distance well-known in coding theory¹, one might draw an analogy between information and distance in order to establish a hierarchy of entropies.

For any vector \mathbf{x} with components $x_i, i = 1, \dots, N$, its distance from origin or norm is defined according to the following ℓ_p -norm formula:

$$\|\mathbf{x}\|_p = \left(\sum_{i=1}^N |x_i|^p \right)^{\frac{1}{p}} \quad (\text{D2})$$

Thus: $\|\mathbf{x}\|_1 = \sum_{i=1}^N |x_i|$ is the ℓ_1 -norm, whereas the ordinary Euclidean norm is $\|\mathbf{x}\|_2 = \left(\sum_{i=1}^N |x_i|^2 \right)^{\frac{1}{2}}$ the ℓ_2 -norm. Taking the case $p \rightarrow \infty$ we get the Infinity norm ℓ_∞ with $\|\mathbf{x}\|_\infty = \max_{i=1 \dots N} |x_i|$. Mathematically, the three norms are equivalent, however computationally wise, ℓ_∞ norm is the most efficient in terms of number of arithmetic operations.

In the entropy case, we define the order $q \in [0, \infty[$ Rényi function:

$$R_q = \frac{1}{1-q} \log_2 \left(\sum_{i=1}^N p_i^q \right) \quad (\text{D3})$$

The Rényi entropy is additive like Shannon's and for $q \rightarrow 1$, they are same:

$$\begin{aligned} R_1 &= \lim_{q \rightarrow 1} R_q = - \frac{d}{dq} \left(\log_2 \left(\sum_{i=1}^N p_i^q \right) \right)_{q=1} \\ &= - \sum_{i=1}^N p_i \log_2 p_i \equiv H_S \end{aligned} \quad (\text{D4})$$

Using the analogy with the Infinity norm ℓ_∞ , we obtain the min-entropy as:

$$R_\infty = - \max_{i=1 \dots N} \log_2 p_i \quad (\text{D5})$$

Similarly to the ℓ_∞ norm, the Rényi entropy is very efficient, computationally wise.

Considering for an example, Poisson distributed photons⁵⁰, with mean $\langle n \rangle$ and probabilities $p_i = \frac{e^{-\langle n \rangle} \langle n \rangle^i}{i!}$, Shannon entropy is given by:

$$H_S = \frac{1}{2} \log_2 (2\pi e \langle n \rangle) \quad (\text{D6})$$

In comparison, the min-entropy is obtained after estimating $\max_{i=1 \dots N} \{p_i\}$ and that occurs when $i \approx \lfloor \langle n \rangle \rfloor$, the integer part of $\langle n \rangle$, thus:

$$R_\infty = - \log_2 \left[\frac{e^{-\langle n \rangle} \langle n \rangle^{\lfloor \langle n \rangle \rfloor}}{\lfloor \langle n \rangle \rfloor!} \right] \quad (\text{D7})$$

Entropy hierarchy is represented by the inequalities $0 \leq R_\infty \leq R_q \leq H_S \leq R_{q'}$ (with $q > 1$ and $0 < q' < 1$). In the case of perfectly random n -bit strings, both entropies H_S and R_∞ per bit are equal to one, since $p_i = 1/N, \forall i$ with $N = 2^n$ and $\max_{i=1 \dots N} \{p_i\} = 1/N$.

¹ A. B. Carlson and P. B. Crilly *Communication systems: An Introduction to Signals and Noise in Electrical Communication*, 5th Edition, McGraw-Hill, New York (2010).

² H. Nyquist, "Thermal agitation of electric charge in conductors," *Phys. Rev.* **32**, 110 (1928). See also J. B. Johnson, *Phys. Rev.* **32**, 97 (1928).

³ A. A. Penzias and R. W. Wilson, "A measurement of excess antenna temperature at 4080 Mc/s" *Astrophys J.* **412**, 419 (1965). See also: R.H. Dicke, P.J.E. Peebles, P.G. Roll and D.T. Wilkinson "Cosmic blackbody radiation" *Astrophys J.* **412**, 414 (1965).

⁴ B. Yurke and J. S. Denker "Quantum Network Theory", *Phys. Rev. A* **29**, 1419 (1984).

⁵ Wave-particle duality applied to massless photons is due, surprisingly, to Einstein. De Broglie used duality for massive particles and considered that the photon had a finite mass.

⁶ H. Schmidt, *J. App. Phys.*, **41**, 462 (1970).

⁷ A. Einstein, B. Podolsky, and N. Rosen, *Phys. Rev.* **47**,

777 (1935).

⁸ E. Schrödinger, *Proc. Cambridge Philos. Soc.* **31**, 555 (1935); **32**, 446 (1936).

⁹ J. S. Bell, *Physics* **1**, 195 (1964).

¹⁰ F. Buscemi, *Phys. Rev. Lett.* **108**, 200401 (2012).

¹¹ In Analytical Mechanics, a degree of freedom corresponds to a generalized coordinate (e.g. for a gas containing N particles moving in d dimensions, the number of degrees of freedom is Nd). In Statistical Mechanics, if the energy contains g quadratic terms, g is the number of degrees of freedom and the mean energy is $gk_B T/2$ (see for instance J. D. Walecka, *Fundamental Statistical Mechanics: Manuscript and Notes of Felix Bloch*, Imperial College Press and World Scientific, 2000). More generally, when the energy is homogeneous of order ν in g variables, its mean value is $gk_B T/\nu$. Mathematically, when the Hamiltonian is such that $H(\lambda\xi_1, \lambda\xi_2, \dots, \lambda\xi_g, \xi_{g+1}, \dots) = \lambda^\nu H(\xi_k)$, where λ is an arbitrary real number, it is homogeneous of order ν in the g variables $\{\xi_1, \xi_2, \dots, \xi_g\}$. Note that Reif¹² and Landau-

- Lifshitz¹³ definitions of degrees of freedom conform to the Analytical Mechanics case.
- ¹² F. Reif, *Statistical and Thermal Physics*, McGraw-Hill, New-York (1985).
- ¹³ L. D. Landau and E. M. Lifshitz, *Statistical Physics*, Vol. 5, Pergamon, Oxford (1975).
- ¹⁴ I. S. Gradshteyn and I. M. Ryzhik, *Table of Integrals, Series and Products*, Academic Press, New-York (1980).
- ¹⁵ C. W. Gardiner, *Handbook of Stochastic Methods*, 2nd ed. (Springer-Verlag, Berlin, 1990).
- ¹⁶ The factor 2 discrepancy ($4Rk_B T$ versus $2Rk_B T$) occurring in the PSD $S_V(\omega)$ or in the voltage fluctuation σ_V^2 is resolved by multiplying by 2 the contributions for positive and negative ω .
- ¹⁷ H.B. Callen and T.A. Welton, *Phys. Rev.* **83**, 34 (1951).
- ¹⁸ M. Campisi, P. Hänggi, and P. Talkner, "Quantum fluctuation relations: Foundations and applications", *Rev. Mod. Phys.* **83**, 771 (2011).
- ¹⁹ M. Planck, *Annalen der Physik (Leipzig)* **37**, 642 (1912).
- ²⁰ In modern statistical physics language, the classical limit is obtained when the Bose-Einstein factor $\langle n \rangle = \frac{1}{e^{\beta(\hbar\omega - \mu)} - 1} \ll 1$ with μ the chemical potential or when mean particle distance is much larger than thermal wavelength¹³. When $\beta\mu \rightarrow -\infty$, we recover Boltzmann distribution $\langle n \rangle \approx e^{-\beta(\hbar\omega - \mu)}$. The photon number not being conserved, $\mu = 0$ for all temperatures, implying that the photon character is always quantum and the "classical" limit $k_B T \gg \hbar\omega$ invoked by Planck bypasses the quantum nature of the photon.
- ²¹ L. D. Landau and E. M. Lifshitz, *Quantum Mechanics*, Vol. 3, Pergamon, Oxford (1965).
- ²² The classical contribution to energy from the equipartition theorem is $2 \times 2 \times \frac{1}{2} k_B T = 2k_B T$ since the electromagnetic oscillator energy per mode is quadratic with respect to two orthogonal field components (electric and magnetic) and two polarizations (right and left circular) are present. The polarization contribution is in the prefactor $2 \times \frac{\omega^2}{\pi^2 c^3}$ which is same for both Rayleigh-Jeans and Planck expressions of the photon spectral density.
- ²³ A. A. Clerk, M. H. Devoret, S. M. Girvin, F. Marquardt, and R. J. Schoelkopf, "Introduction to quantum noise, measurement, and amplification" *Rev. Mod. Phys.* **82**, 1155 (2010).
- ²⁴ H. Goldstein, *Classical Mechanics*, Addison-Wesley, New-York (1980).
- ²⁵ W. H. Press, W. T. Vetterling, S. A. Teukolsky and B. P. Flannery, *Numerical Recipes in C: The Art of Scientific Computing* Third Edition, Cambridge University Press, New-York (2007).
- ²⁶ Knuth, D.E. 1981, *Seminumerical Algorithms*, 2nd ed., *The Art of Computer Programming* vol. 2 (Addison-Wesley).
- ²⁷ G-B Stan, J-J Embrechts and D. Archambeau, *Comparison of Different Impulse Response Measurement Techniques*, *J. Audio Eng. Soc.* **50**, 249 (2002).
- ²⁸ A. Ekert and R. Renner "The ultimate physical limits of privacy" *Nature*, **507**, 443 (2014).
- ²⁹ V. Scarani, H. Bechmann-Pasquinucci, N. J. Cerf, M. Dušek, N. Lütkenhaus and M. Peev, *Rev. Mod. Phys.* "The security of practical quantum key distribution" **81**, 1304 (2009).
- ³⁰ Continuous variable quantum information processing corresponds to the quantum version of the analog computer. A simple representative variable is $|x\rangle$ the position representation eigenstate, a continuous version of the qubit that belongs to an infinite dimensional Hilbert space.
- ³¹ Mathematically, a spinor reverses its sign when the polar angle is rotated by 2π since $|\psi(\theta + 2\pi, \phi)\rangle = \hat{R}_z(\theta + 2\pi, \phi) |\psi(\theta, \phi)\rangle = -|\psi(\theta, \phi)\rangle$
- ³² J. L. O'Brien, A. Furusawa and J. Vučković, "Photonic quantum technologies", *Nature Photonics*, **3**, 687 (2009).
- ³³ B. Julsgaard, A. Kozhekin and E. S. Polzik, "Experimental long-lived entanglement of two macroscopic objects", *Nature*, **413**, 400 (2001).
- ³⁴ P. G. Kwiat, K. Mattle, H. Weinfurter and A. Zeilinger, *Phys. Rev. Lett.* **75**, 4337 (1995).
- ³⁵ D. L. Moehring, P. Maunz, S. Olmschenk, K. C. Younge, D. N. Matsukevich, L.-M. Duan and C. Monroe, "Entanglement of single-atom quantum bits at a distance", *Nature*, **449**, 68 (2007).
- ³⁶ R. Colbeck and R. Renner, *Nature Physics* **8**, 450 (2012).
- ³⁷ B. Sanguinetti, A. Martin, H. Zbinden and N. Gisin, *Phys. Rev. X* **4**, 031056 (2014).
- ³⁸ T. M. Cover and J. A. Thomas, *Elements of Information Theory*, 2nd edition, Wiley, New-York (2006).
- ³⁹ C. Gobby, Z. L. Yuan and A. J. Shields, *App. Phys. Lett.* **84**, 3762 (2004).
- ⁴⁰ H-K Lo, X. Ma and K. Chen, *Phys. Rev. Lett.* **94**, 230504 (2005).
- ⁴¹ L. C. Comandar, B. Frohlich, M. Lucamarini, K. A. Patel, A. W. Sharpe, J. F. Dynes, Z. L. Yuan, R. V. Pentyl and A. J. Shields, *App. Phys. Lett.* **104**, 021101 (2014).
- ⁴² S. Ritter, C. Nölleke, C. Hahn, A. Reiserer, A. Neuzner, M. Uphoff, M. Mücke, E. Figueroa, J. Bochmann, and G. Rempe "An elementary quantum network of single atoms in optical cavities" *Nature*, **484**, 195 (2012).
- ⁴³ D. Reitz, C. Sayrin, R. Mitsch, P. Schneeweiss, and A. Rauschenbeutel, *Phys. Rev. Lett.* **110**, 243603 (2013).
- ⁴⁴ J-C Forgues, C. Lupien, and B. Reulet, *Phys. Rev. Lett.* **114**, 130403 (2015).
- ⁴⁵ In the low-temperature experiment performed at 18 mK, the junction is subjected to a magnetic field forbidding Aluminum to become superconducting: Al has 0.01 T critical field and 1.2 K critical temperature.
- ⁴⁶ N. Kalb, A. Reiserer, S. Ritter and G. Rempe, *Phys. Rev. Lett.* **114**, 220501 (2015).
- ⁴⁷ H.B. Callen *Thermodynamics and an introduction to thermostatistics*, 2nd edition, Wiley, New-York (1985).
- ⁴⁸ C. Kittel, *Introduction to Solid State Physics*, Wiley, New-York (1975).
- ⁴⁹ E. Wigner, *Annals of Mathematics*, **40**, 149 (1939).
- ⁵⁰ R. Appledorn, *SIAM Review* **30**, 314 (1988).